

PROCEEDINGS OF SPIE

[SPIDigitalLibrary.org/conference-proceedings-of-spie](https://spiedigitallibrary.org/conference-proceedings-of-spie)

The Visible Telescope onboard the Chinese-French SVOM satellite

Fan, Xuewu, Zou, Gangyi, Wei, Jianyan, Qiu, Yulei, Gao, Wei, et al.

Xuewu Fan, Gangyi Zou, Jianyan Wei, Yulei Qiu, Wei Gao, Wei Wang, Wengang Yang, Jian Zhang, Chuang Li, Hui Zhao, Lijun Dan, Zongxi Song, Liangjie Feng, Guorui Ren, Chao Huang, Hao Yuan, Zhonghan Sun, Fengtao Wang, Chenjie Wang, Wei Li, Chao Shen, Ning Qi, Yue Pan, "The Visible Telescope onboard the Chinese-French SVOM satellite," Proc. SPIE 11443, Space Telescopes and Instrumentation 2020: Optical, Infrared, and Millimeter Wave, 114430Q (13 December 2020); doi: 10.1117/12.2561854

SPIE.

Event: SPIE Astronomical Telescopes + Instrumentation, 2020, Online Only

The Visible Telescope onboard the Chinese-French SVOM Satellite

Xuewu Fan^a, Gangyi Zou^{*a,b}, Jianyan Wei^c, Yulei Qiu^c, Wei Gao^a, Wei Wang^a, Wengang Yang^a, Jian Zhang^a, Chuang Li^a, Hui Zhao^a, Lijun Dan^a, Zongxi Song^a, Liangjie Feng^a, Guorui Ren^a, Chao Huang^a, Hao Yuan^a, Zhonghan Sun^a, Fengtao Wang^a, Chenjie Wang^a, Wei Li^a, Chao Shen^a, Ning Qi^a, Yue Pan^{a,b}

^a Space Optics Laboratory, Xi'an Institute of Optics and Precision Mechanics, Chinese Academy of Sciences, Xi'an 710119, China

^b University of Chinese Academy of Sciences, Beijing 100049, China

^c National Astronomical Observatories, Chinese Academy of Sciences, Beijing 100012, China

ABSTRACT

The Space-based multi-band astronomical Variable Objects Monitor (SVOM) project is a dedicated satellite developed at the cooperation of China and France, aim to make prompt multi-band observations of Gamma-Ray Bursts (GRBs), the afterglows and other high-energy transient astronomical events. The Visible Telescope (VT) is one of the four payloads onboard the SVOM. VT is designed to observe the afterglows of GRBs both in the visible and near infrared bands simultaneously. The telescope can reach a limiting magnitude of +22.5Mv and provide the redshift indicators for high-Z ($z > 4$) GRBs. VT is also designed to measure the Relative Performance Errors (RPEs) for the satellite attitude and orbit control system (AOCS), aiming to improve the pointing stability of the platform during observation. VT adopts a Ritchey-Chrétien (RC) catadioptric optical configuration with a 440mm aperture and uses the dichroic prism before the focal plane to split the incident light into blue (visible) and red (near infrared) band. Two Fine Guidance Sensor (FGS) CCDs are mounted beside the main CCD on the blue band focal plane of VT and provide sub-arcsecond pixel resolution. Fiber reinforced plastic (CFRP) composites is selected as the material of VT's main structure to ensure enough stiffness and strength during launch. The electrical video processing circuit is carefully designed to make the readout noise below 6e-/pix (rms) in 100s exposure time. Active and passive thermal control are used together to ensure the optical performance and thermoelectric cooler (TEC) is adopted to control the main CCDs working temperature below -65°C to reduce the noise. This paper provides a comprehensive overview of the scientific requirements and the key instrument design aspects of optics, main structure, electrics, thermal control, performance test and validation results of VT.

Keywords: GRBs, SVOM, VT, RC catadioptric, FGS, CFRP, TEC

1. INTRODUCTION

Gamma-ray bursts are brief, extremely bright flashes detected out to cosmological distances. The initial blast is followed by an afterglow, which can continue for as long as months, providing important clues as to the nature of these explosive events. SVOM is a Sino-French mission dedicated to detection, localization and broadband observation of Gamma-Ray Bursts (GRBs) to study their extreme physics and use them for cosmology^[1]. SVOM will also be devoted to the multi-messenger astronomy era. Between alerts, an ambitious program will be devoted to various classes of high-energy or variable phenomena, like X-ray bursts, soft gamma repeaters, Active Galactic Nuclei (AGN), novae, and supernova.

The mission requirements from the SVOM Science Team are summarized below^[2]:

- ✓ Permit the detection of all known types of GRBs
- ✓ Provide fast, reliable GRB positions
- ✓ Measure the broadband spectral shape of the prompt emission (from visible to MeV)
- ✓ Measure the temporal properties of the prompt emission (from visible to Mev)

*zougangyi@opt.ac.cn

Space Telescopes and Instrumentation 2020: Optical, Infrared, and Millimeter Wave, edited by
Makenzie Lystrup, Marshall D. Perrin, Proc. of SPIE Vol. 11443, 114430Q · © 2020 SPIE
CCC code: 0277-786X/20/\$21 · doi: 10.1117/12.2561854

- ✓ Quickly identify the afterglows of detected GRBs at X-ray and optical wavelengths, including those which are highly redshifted ($z > 4$)
- ✓ Measure the broadband spectral shape of the early and later afterglow (from visible to X-rays)
- ✓ Measure the temporal evolution of the early and later afterglow (from visible to X-rays)

SVOM will be launched in 2022 on a Low Earth Orbit ($h=630\text{km}$, $i=30$)^[3], providing a qualitative leap forward in our ability to study bursts. SVOM payload is composed of a set of different instruments:

- ✓ ECLAIRs, a hard X-ray camera which triggers on GRBs present within its field of view (FOV) in the hard X-ray energy range^[4].
- ✓ Gamma-Ray Monitor (GRM), a γ -ray spectrometer, which observes simultaneously the same field of view in the γ -ray energy range.
- ✓ Micro channel X-ray Telescope (MXT), a narrow-field X-ray telescope to quickly observe the error boxes provided by the hard X-ray imager^[5].
- ✓ Visible Telescope (VT), a narrow-field visible telescope to quickly observe the error boxes provided by the hard X-ray imager.

And a set of ground-based instruments^[5]:

- ✓ Two GFTs, Ground Follow-up robotic Telescopes (C-GFT and F-GFT)
- ✓ GWAC, an array of Wide-Field optical cameras monitoring the field of view (FOV) of ECLAIRs

And a ground segment in charge of the monitoring of the scientific payload and the alert system.

The ECLAIRs imager, and the associated GRM observe jointly a large portion of the sky (2 Sr). The ECLAIRs data processing unit analyzes the counts recorded by the detection plane in real time, in order to detect and localize GRBs occurring within its FOV. Upon detection of a new source candidate, an alert is transmitted as quickly as possible to the ground via the VHF real-time network and relayed to the international community by the French Science Center (FSC). In 65% of the cases, the first position is expected to reach the ground 30 seconds after it has been derived on-board. If the detection is significant enough, the GRB position is transmitted to the platform for an autonomous satellite slew^[6] (within five minutes) that will bring the GRB within the field of view of the narrow-field instruments: the MXT and VT telescopes. The narrow field instruments detect the GRB position and permit the study of the early afterglow. If these instruments detect the afterglow, SVOM will generate alerts containing the X-ray position of the afterglow (sub arcmin), and possibly the optical position computed from VT data (around one arcsec). These alerts will reach the community within 10 minutes from the first alert.

Two SVOM 1m class robotic telescopes will automatically position their 20-30 arcmin wide field-of-view onto the position of the GRB alert and, in case of detection, they will determine the position of the source with 0.5 arc-second accuracy and deliver a redshift estimate. It will ensure the vital link between the SVOM alerts and the largest facilities (VLT, E-ELT and ALMA at ESO, IRAM, GTC, etc.), which cannot be triggered without a precise localization due to their narrow field of view.

2. OVERALL DESCRIPTION

The main task of VT is to observe the afterglows of GRBs both in the visible and near infrared and provide redshift estimation and some promising candidates at the early time for the ground based large telescopes. Another task of VT is to measure the Relative Performance Error (RPE) of the satellite, aiming to improve the pointing stability of the platform during observation. Two additional Fine Guidance Sensors (FGSs) are mounted on the visible focal plane of VT besides the main CCD to measure the image shifts and rotations. As illustrated in Figure 1, VT is mounted on the SVOM optical bench with the ECLAIRs, the GRMs and the MXT.

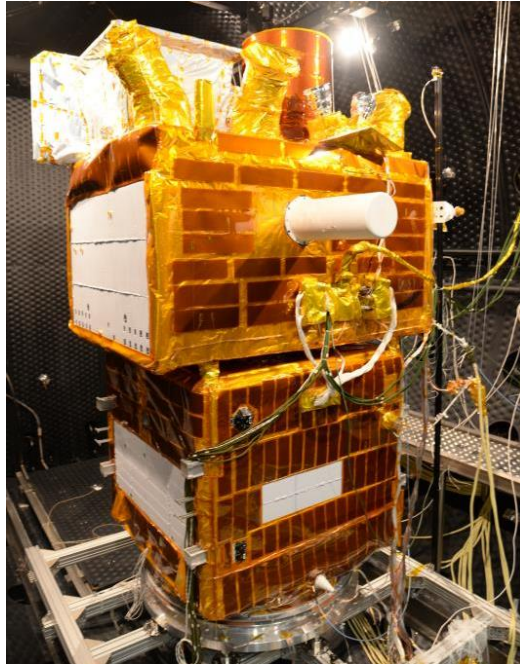


Figure 1. SVOM in a class 10 000 cleanroom during the integration and test phase at Shanghai. The four instruments are mounted on the optical bench with several of the electronics boxes and the sun-shield. The solar arrays are not yet installed.

2.1 Science requirements

The space-borne Visible Telescope should fulfill the following requirements:

- ✓ To improve the GRB localizations obtained by the ECLAIRS and MXT to sub-arcsecond precision through the observation of the optical afterglow
- ✓ To obtain a deep and uniform light-curve sample of the optical afterglow
- ✓ To do primary selection of optically dark GRBs and high-redshift GRB candidate ($z > 4$)

The field of view of the telescope should be large enough to cover the error box of the ECLAIRS localization. The detecting area of the CCD has 2048×2048 pixels to ensure the sub-arcsecond localization of the detected sources. A frame-transfer CCD is preferred in order to minimize the dead time.

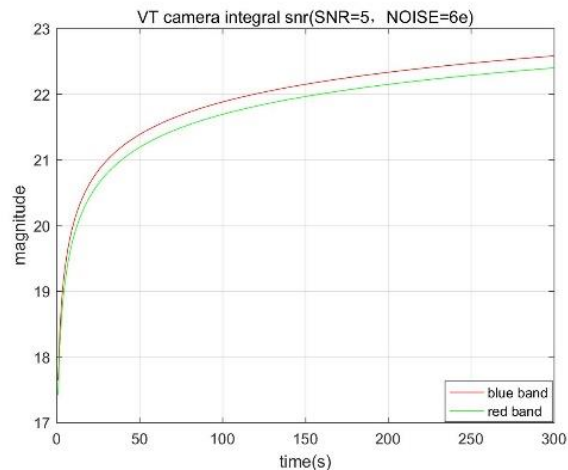


Figure 2. The sensitivity of VT

The aperture of the telescope should guarantee a limiting magnitude of $M_v=22.5$ (5σ) for 300 sec equivalent exposure time. Such a sensitivity is a significant improvement over the UVOT onboard the Swift satellite^[7]. It is expected to allow for the telescope to detect nearly 70% of SVOM GRBs during the first orbit and, for the first time, to explore the realm of ‘dark GRBs’. The sensitivity of the telescope is given in Figure 2. The telescope should have at least two bands in order to select high-redshift GRB candidates. The two bands are separated at 650nm, which corresponds to a redshift of $z\sim 4-4.5$ using Ly α absorption as the redshift indicator.

2.2 VT specifications

Tables of VT and FGS instrument parameters are listed in Table 1 and Table 2 respectively.

Table 1. The specifications of VT

| Parameters | Description |
|--------------------------------|--|
| Sensitivity | $M_v=22.5$ (3sigma, 300s exposure) |
| Pixel resolution | 0.77arcsecond/pixel |
| Pupil diameter | 440mm |
| Focal length | 3600mm |
| Field of view | $\geq 26\text{arcmin} \times 26\text{arcmin}$ |
| Spectral range | 400nm~650nm (blue band): 650nm~1000nm (red band) |
| Surface obscuration | 0.18 |
| Optical transmission | 0.6(average) |
| Detector | 2048×2048 pixels, 13.5um×13.5um |
| Diameter of 80% EE (blue band) | ≤ 2 pixels |
| Diameter of 70% EE (red band) | ≤ 2 pixels |
| CCD working temperature | $-65^\circ \pm 2^\circ\text{C}$ (blue band); $-75^\circ \pm 2^\circ\text{C}$ (red band); |
| ADC | 16bits |
| Readout noise | $< 8e^-/\text{pix}$ (15s, 30s exposure time) ; $< 6e^-/\text{pix}$ (100s, 300s exposure time) |
| Stray light | $< 1/3$ sky background when the Moon is $> 30\text{deg}$ off axis. |

Table 2. The specifications of FGS

| Parameters | Description |
|--------------------------------|--|
| Field of View | $12.7^\circ \times 12.7^\circ$ |
| Spectral range | 400-650nm |
| Detector | 1024×2048 pixels (back-illuminated, frame transfer), 13um×13um |
| Diameter of 80% EE (blue band) | ≤ 3 pixels |
| CCD working temperature | -20°C (blue band) |
| ADC | 14bits |
| Readout noise | $< 10e^-/\text{pix}$ |

2.3 Overall description

The VT is made up of 5 functional units (see Figure 3): VT main body, image processing box, primary control box, TEC control box and thermal control box^[8].

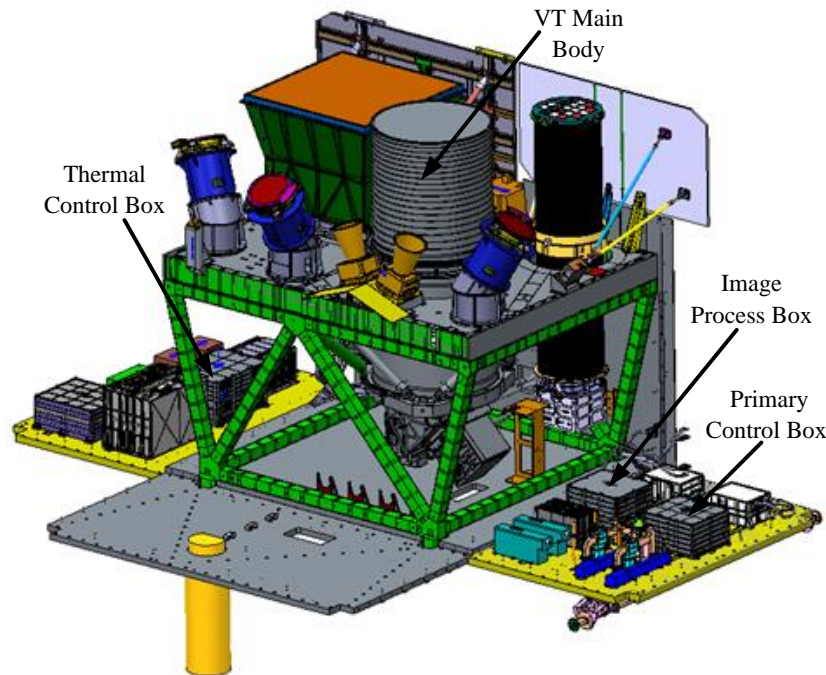


Figure 3. VT inside the Payload Module of SVOM

The VT main body is composed of optics and its metering structure, focalization mechanism, calibration door and baffles. The optical system of VT adopts a Ritchey-Chrétien (RC) configuration with three dedicated lenses and an ingenious dichromatic ray-splitting prism. The first two lenses are servo-controlled along the optical axis to adjust focus which is necessary for VT to keep the optical performance in orbit. Then an ingenious dichroic prism ray-splitter is inserted before the focal plane to ensure VT can take observations in the blue band and red band simultaneously.

The two main band CCDs (red: CCD42-80, blue: CCD42-80) are placed at the center of field. Two fine guidance sensors (FGSs, CCD47-20) are mounted on the blue band focal plane of VT along the main CCD (CCD 42-80) (see Figure 4) ^[11].

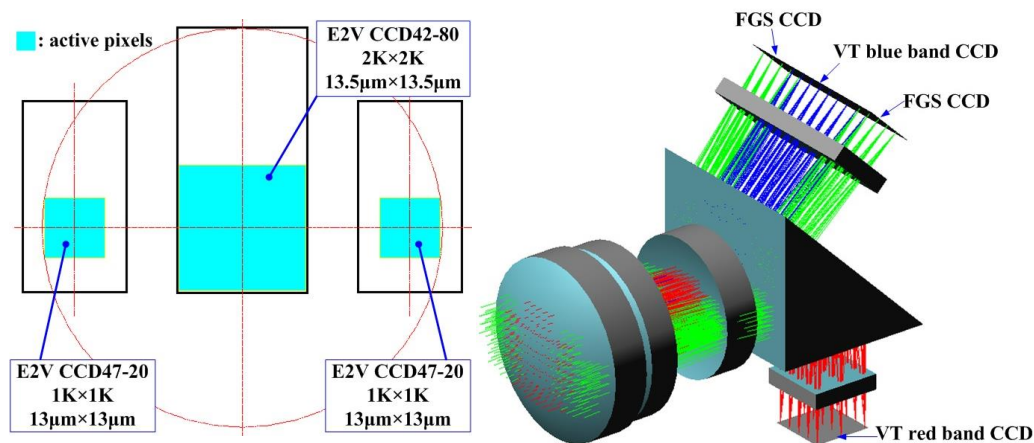


Figure 4. CCDs arrangement (left) and positions (right) on the blue band focal plane

The calibration door is placed before the third lens. 36 LEDs are set up along the door. In order to suppress stray light, three baffles are designed: the primary mirror's inner baffle, the outside baffle of the secondary mirror and the external baffle ^[9-10].

The Electronics of VT consists of five parts: electric box, video processing box, FPA box, thermal control box and TEC control box.

3. INSTRUMENT DESCRIPTION

3.1 Optics^[11]

VT optical system is adopted a modified Ritchey-Chrétien (RC) catadioptric design configuration, which is shown in Figure 5. It contains a 440mm primary and 135mm secondary mirror, which are both made of Silicon Carbide (SiC). Behind the primary mirror is the three lenses. The first two lenses are servo-controlled along the optical axis to adjust focus which is necessary for VT to keep the optical performance in orbit. Then an ingenious dichroic ray-splitting prism is inserted before the focal plane to ensure VT can take observations in the blue band and red band simultaneously. The vacuum windows for ground performance tests are also taken into consideration. Fused silica is used for the first lens and vacuum windows, while HLAk3 is used for the other two lenses and HZK3 is used for the prism. All the glass materials are radiation proof for space application.

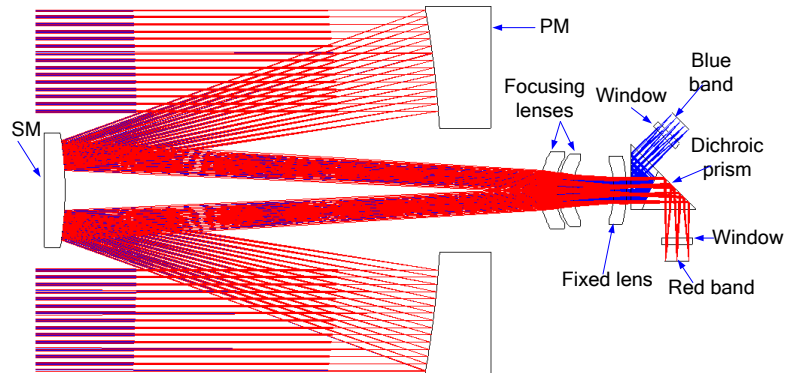


Figure 5. Schematic optics layout of VT

In order to improve the pointing precision of the satellite attitude control system, two fine guidance sensors (FGSs) are mounted on the blue band focal plane of VT. The preferred CCD for VT is the back-illuminated high performance E2V CCD42-80 full frame CCD without window, which operates in frame transfer mode. The pixel size is $13.5\mu\text{m}\times 13.5\mu\text{m}$ and the array size is $2\text{K}\times 2\text{K}$. E2V CCD47-20 has been chosen to be the FGS sensor, whose pixel size is $13\mu\text{m}\times 13\mu\text{m}$ and the array size is $1\text{K}\times 1\text{K}$. CCD47-20 has a 1.5mm-thick NBK7 window. The CCDs arrangement on the focal plane is shown in Figure 4. The minimum diameter of the circle that enclosed the CCDs is 87.69mm, so the design circular field of view (FOV) of VT should be no less than 1.39° . Finally, the design circular FOV of VT is 1.4° for blue band, while the design circular FOV for red band is 0.63° .

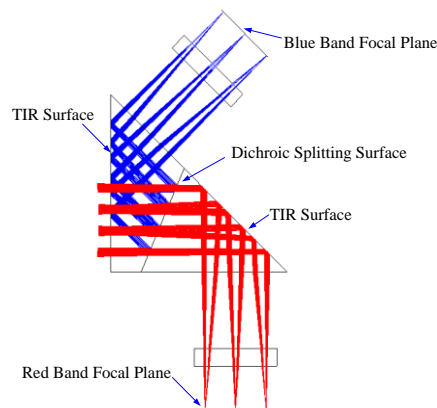


Figure 6. Prism design and ray splitting concept

Figure 6 shows the dichroic ray-splitting method. It is just like a 45° right angle prism, divided into a half-penta prism and the remain part. The rays of blue band are reflected, while the rays of red band are refracted at the dichroic splitting surface. The glass type of the prism has been selected carefully to make sure the beam can be totally internal reflected (TIR) at the TIR surface.

Distances between optical elements have been managed to achieve a satisfactory package. The final design envelope is $\Phi 450\text{mm} \times 760\text{mm}$, excluding the external baffle. To reduce the light loss due to the central obscuration, the diameter of SM has been minimized to about 30% (in diameter), with respect to the PM.

3.2 Structure

Structural concept of VT is shown in Figure 7, which consists of primary mirror assembly, telescope support plate assembly, secondary mirror assembly, barrel assembly, interface strut components, outside baffle, after optics assembly, focalization mechanism, CCD boxes, electronic boxes, and thermal control components, etc.

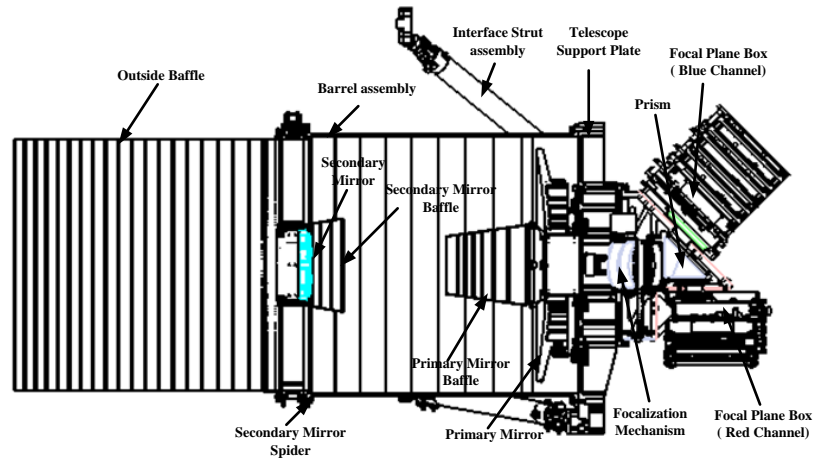


Figure 7. The main body structure of VT

Telescope support plate (TSP) assembly: TSP is the primary structural element of the VT and is responsible for supporting the forward and aft telescope tubes, the primary mirror module and the focal plane box. It also provides the interface to the SVOM optical bench.

Barrel assembly: The 500mm diameter carbon fiber tube is made of CFRP meters the support plane and the secondary mirror spider.

Interface strut components: VT is mounted on the deck of the PIM with interface strut assembly. The interface strut assembly is made up of a hexapod with 6 struts as legs and 3 titanium alloy brackets as the interface between the struts and the PIM.

Calibration mechanism: CM is mounted on the support structure of the aft optics system. The calibration mechanism includes a diffuser plate between the second lens and the third lens, worm couple, step motor, and potentiometer, shown in Figure 8. The diameter of the diffuser plate is 80mm with a thickness of 1mm. The diffuser plate was made of aluminum alloy, machined to required roughness. The calibration LEDs will be laid around the third lens.



Figure 8. Picture of the diffuser plate assembly

Focalization mechanism: VT uses lens to adjust focus. FM is made up of worm couple, gear parts, guide rail, ball screw, lens parts, breadboard, step motor, and potentiometer, shown in Figure 9. Using guide rail and spherical lead screw, electric engine makes rotary motion transfer rectilinear movement. Worm couple can reduce loading and would be self-lock in single direction during launching course, while self-locking in another direction is achieved by electric engine. Gear parts assure potentiometer to work in effective dimension $0^{\circ}\sim 345^{\circ}$.

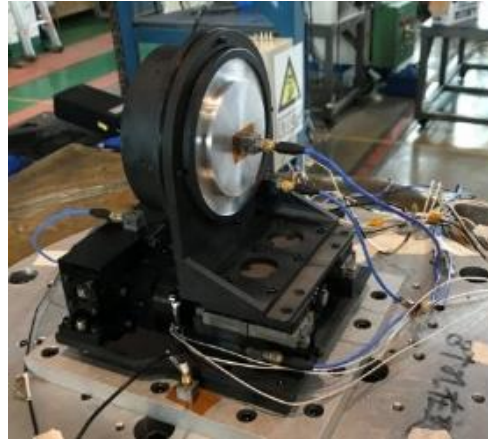


Figure 9. Picture of the focalizing assembly

3.3 Detectors

The four detector assemblies are housed in the Focal Plane Box (FPB). FPB shields the CCDs against trapped protons and cosmic rays and provides cooling for the detector via a coldfinger to the heatpipes. The two cryostats provided vacuum environment in which the CCDs could be cooled for ground testing without moisture. The two cryostats are mounted on the after-optics assembly.

To reduce thermal resistance, the TEC base plate and housing base plate are made of molybdenum which have high thermal conductivity and can match the coefficient of thermal expansion (CTE) of TEC ceramics. Flexible heat pipes are utilized to transfer the heat from the base plate to the radiator. To minimize mechanical load to focal plane assembly to due vibration during launch or in orbit, the heat pipes should have flexible characteristics. The radiator is fixed outside the payload module. VT uses two radiators for different spectrum. The thickness of radiators is 3 mm. The dimension of the radiator for red channel is $533\text{mm} \times 1060\text{mm}$ and the other radiator (for blue channel) is $265\text{mm} \times 1060\text{mm}$ in size.

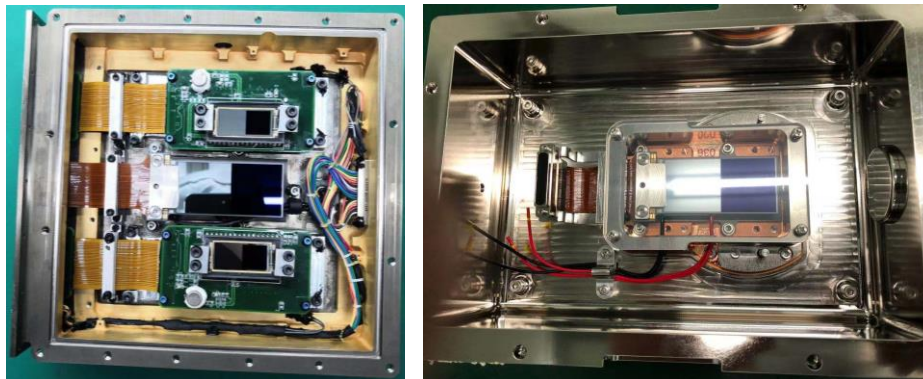


Figure 10. Left: CCDs mounted in the blue band FPB; Right: CCD mounted in the red band FPB.

3.4 Electronics

3.4.1 Focal plane box

Focal plane box contains CCD detector E2V42-80, CCD detector E2V47-20, thermo-electric cooler (TEC), temperature sensor, heater, preamplifier, CCD bias power filter and preamplifier power filter.



Figure 11. The blue band focal plane box

3.4.2 Electric box

Electric box including controlling computer board and secondary power supply board. It uses DC-DC converter to generate all the power supplies used by detection, FGS, FPA and camera control. It sends the direct analogue telemetry signals to satellite power controller, and samples the camera telemetry signals, sends it to PDPU via digital formation. It receives the tele-control command sent by PDPU and sends the camera work parameters to PDPU.



Figure 12. The electric box

3.4.3 Video processing box

Analog processing board, FPGA board, power filter board are included. The timing is designed by the FPGA which generates clocks for CCD, CDS, ADC convert, and controlling signals for the data interface. The FPGA also receives the signals of the controlling computer to change the operational mode of the CCD and the exposure time.

3.4.4 TEC controller

TEC controller contains TEC controlling computer board and TEC secondary power supply board. The temperature range of the CCDs are controlled in $-65^{\circ}\text{C}\sim+2^{\circ}\text{C}$ and $-75^{\circ}\text{C}\sim+2^{\circ}\text{C}$ decided by the work mode.

3.4.5 Thermal control box

The thermal control box is used to control the temperature of the whole optical and mechanical system, as well as the focal plane box, shown in Figure 13.

VT has five kinds of software, that is the electric box software, the TEC control software, the temperature control software, the main CCD FPGA software and the FGS FPGA software.

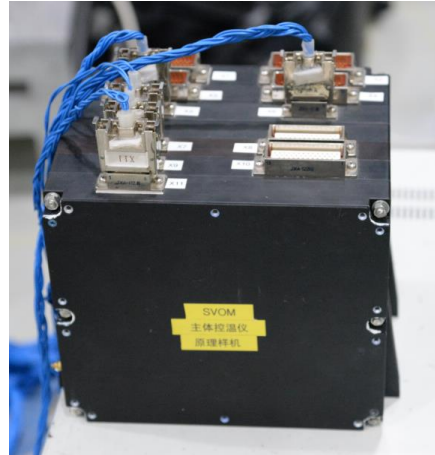


Figure 13. The thermal control box

4. INTEGRATION AND TEST

The subsystems of VT and the SVOM were subjected to the tests outline in Table 3. In order to avoid contamination, the environment of the instrument and spacecraft were controlled throughout the manufacture, integration and environment tests.

Table 3. Tests performed at the various stages of integration

| Instrument Tests | Spacecraft Tests |
|----------------------------------|------------------|
| Opt-mechanical Performance Tests | |
| Electrical Low Noise Tests | |
| Vibration | Vibration |
| Thermal Cycles | Thermal Cycles |
| Thermal Balance | Thermal Balance |
| Calibration | Calibration |
| EMI/EMC | |

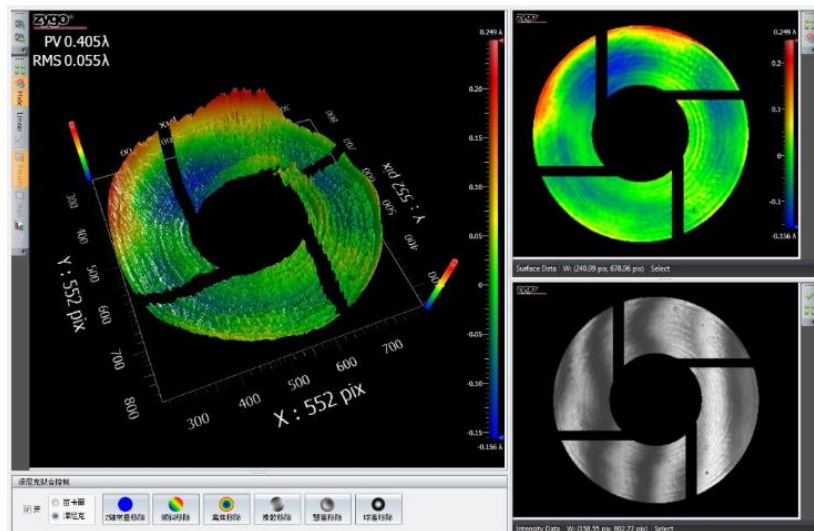


Figure 14. Measured RMS WFE for onaxis FOV of VT

4.1 Optical performance test^[11]

A. RMS WFE test

The RMS WFE of the assembled telescope is measured using a ZYGO interferometer and a flat mirror. The measured RMS WFE of on-axis FOV is 0.055λ ($\lambda=632.8\text{nm}$) which is shown in Figure 14. For the whole FOV, the maximum RMS WFE is 0.06λ . It can be seen that VT has a good optical performance.

B. Encircled energy test

The telescope is finally tested using a collimator with a focal length of 20m in the Lab. A $\Phi 0.02\text{mm}$ star tester is placed on the focal plane of the collimator to simulate a point source in the infinite distance. Figure 15 shows the telescope under EE testing in the Lab.

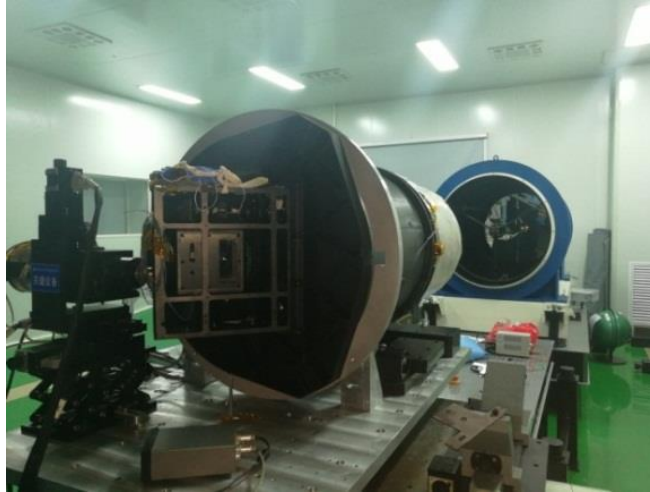


Fig 15. VT under EE testing in the Lab

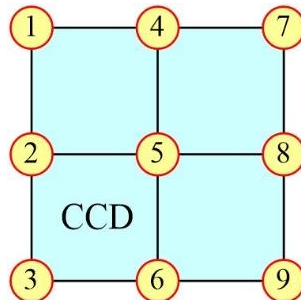


Figure 16. Tested points of FOV on each CCD

Nine FOV points for each CCD are tested (Figure 16). The test results are shown in Table 4. The diameters of 80% (blue band) or 70% (red band) of EE for VT are no more than 1.73 pixels. For FGS, the diameters of 80% EE are all smaller than 2.2 pixels.

Table 4. EE test results for VT and FGS

| FOV points | 1 | 2 | 3 | 4 | 5 | 6 | 7 | 8 | 9 |
|----------------------|------|------|------|------|------|------|------|------|------|
| VT blue band (pixel) | 1.73 | 1.35 | 1.35 | 1.35 | 1.16 | 1.54 | 1.36 | 1.35 | 1.73 |
| VT red band (pixel) | 1.65 | 1.61 | 1.73 | 1.62 | 1.58 | 1.62 | 1.73 | 1.61 | 1.65 |
| FGS1 (pixel) | 2.2 | 1.8 | 1.4 | 1.6 | 1.4 | 1.6 | 1.8 | 1.4 | 1.6 |
| FGS2 (pixel) | 1.8 | 1.8 | 1.8 | 2 | 1.8 | 1.8 | 2 | 1.8 | 2 |

C. PST test

The PST of VT is tested after the opt-mechanical assembling process in the stray light test facility. A collimator with a laser source is employed to simulate the infinite point source. The telescope is put on a rotating table in the double

cylindrical chamber [12, 13]. A stop is located outside the entrance port to prevent the useless light entering the chamber. VT under PST testing in the lab is shown in Figure 17.

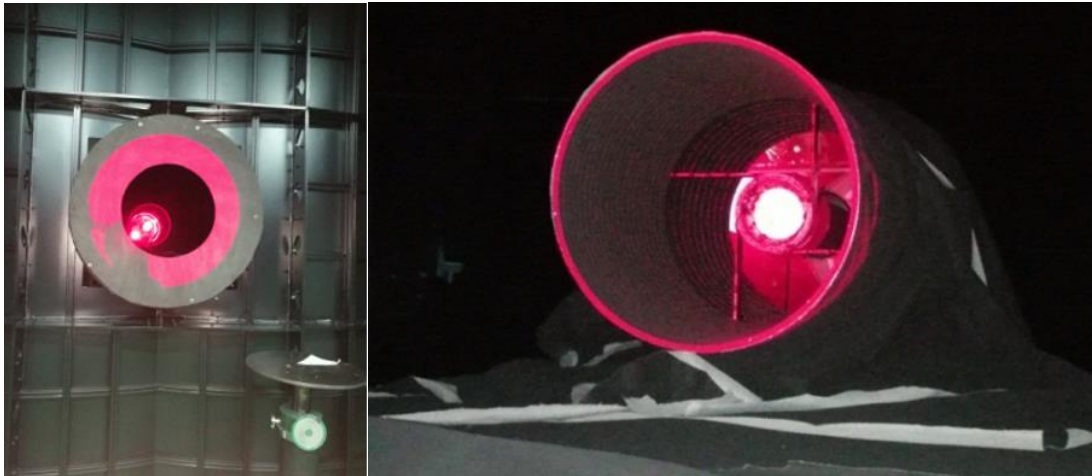


Figure 17. Entrance port of the double cylindrical chamber (left) and VT under PST test (right) in the lab

Figure 18 shows the tested and simulated PST curves for dual band of VT. It can be seen that the tested and simulated PST curves are in good agreement between $\pm 10^\circ$ and $\pm 30^\circ$ off-axis angles. The PSTs at $\pm 30^\circ$ off-axis angle are all less than $2E-7$ for dual band of VT, so the stray light suppression requirement has been met.

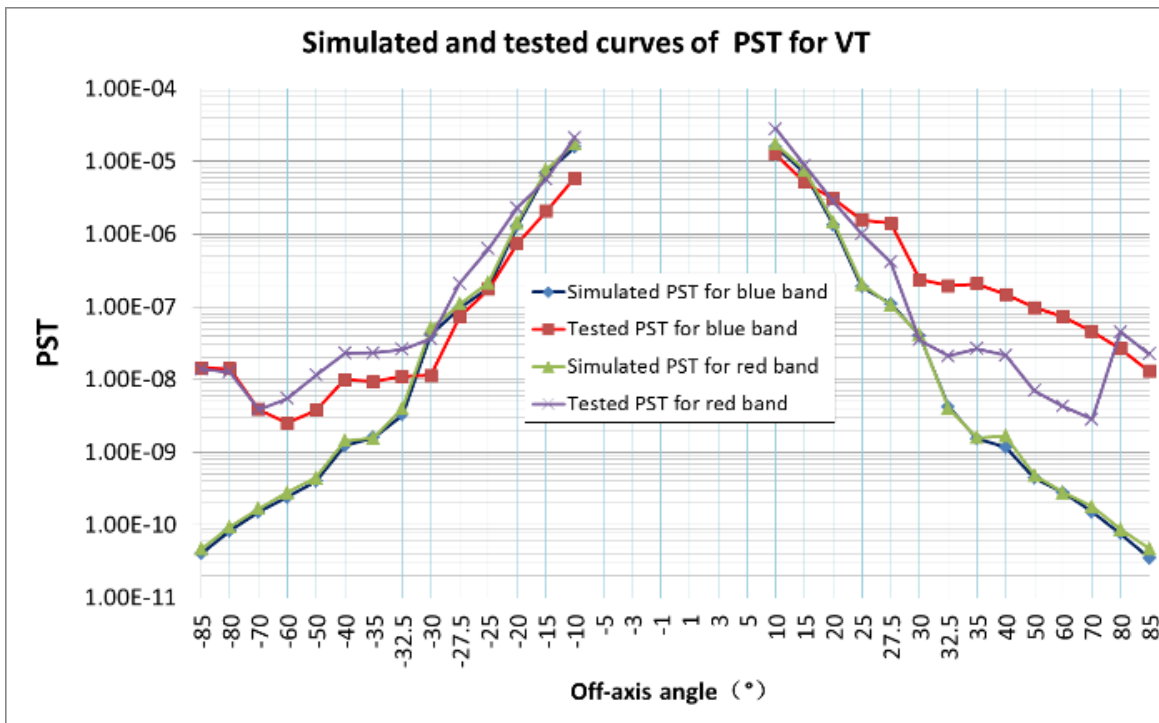


Figure 18. Simulated and tested PST curves for dual band of VT

4.2 Electrical performance test

CCD test bench is established, which is mainly composed of a vacuum chamber, an integrating sphere, light source, monochromator, picoammeter, photodiode and dark box. The vacuum box chamber can provide temperature changes from -170 degrees to +100 degrees, and the vacuum degree is less than 1×10^{-3} Pa, which fully meets the working requirements of the CCD detector.

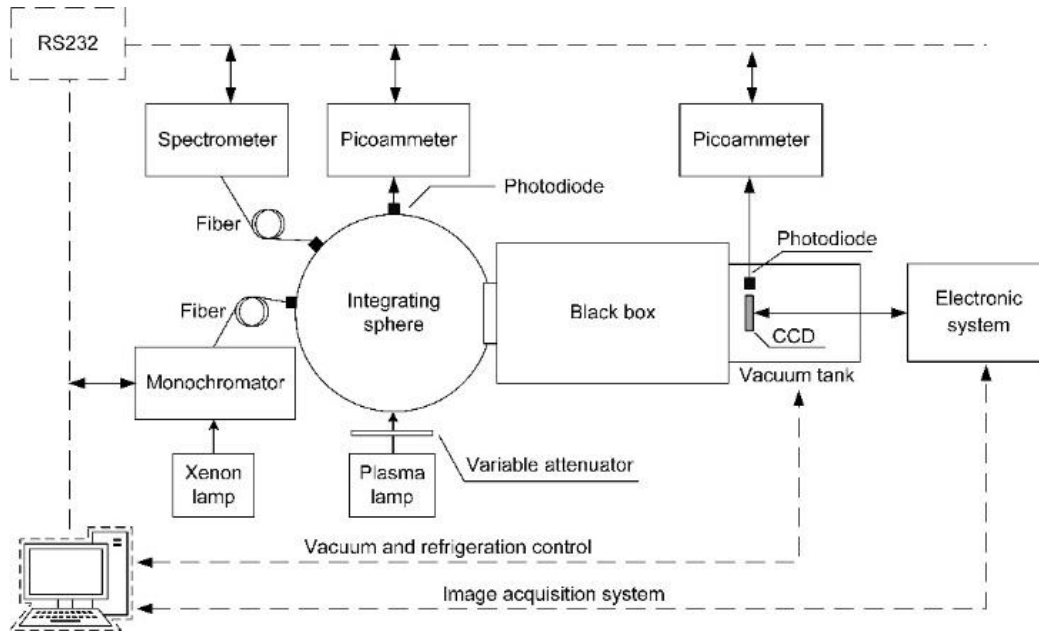


Figure 19. Structure diagram of the CCD test bench

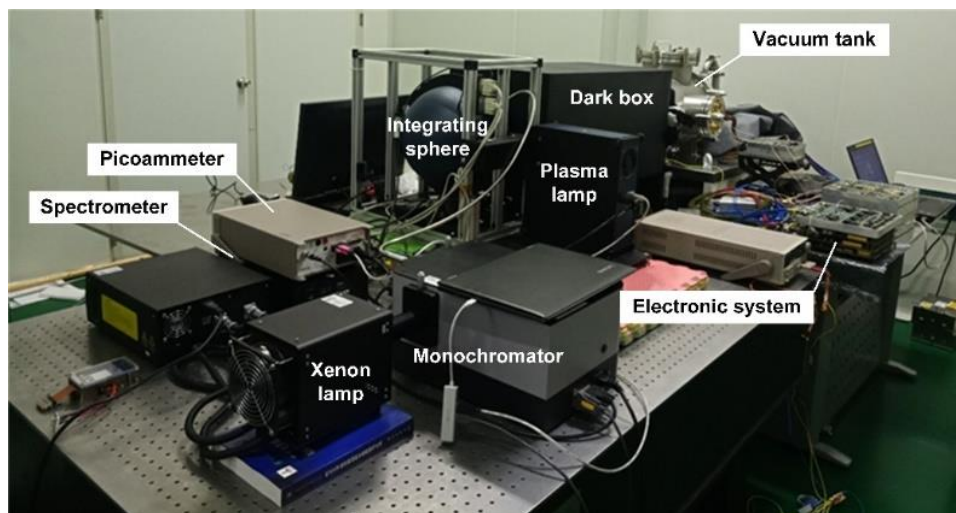


Figure 20. Overview of the CCD test bench

Using the test bench, the main characteristics of three kinds of CCD, including bias field, dark field, flat field, gain, readout noise, quantum efficiency, linearity, etc., have been tested to provide an objective assessment on the performance of the CCD detectors.

The readout noise of AIMO and NIMO-CCD is about $4.7e^{-}$ (@100Khz) and $4.3e^{-}$ (@100Khz) respectively, which is better than its requirement $6e^{-}$. In addition, the dark signals of AIMO-CCD and NIMO-CCD reached $6.8e^{-}$ /pixel/hour and $70.1e^{-}$ /pixel/hour, respectively. And the readout noise and dark signal satisfies the requirement of detecting +22.5Mv targets. The noise of AIMO and NIMO-CCD is about $4.7e^{-}$ (@100Khz) and $4.3e^{-}$ (@100Khz) respectively, which is better than its requirement $6e^{-}$. In addition, the dark signals of AIMO-CCD and NIMO-CCD reached $6.8e^{-}$ /pixel/hour and $70.1e^{-}$ /pixel/hour, respectively. And the readout noise and dark signal satisfies the requirement of detecting +22.5Mv targets.

4.3 Vibration test

VT passed sine vibration and random vibration and shock test (Figure 21). The error of modal frequency between the test value and the analysis value is less than 5%. New design schemes and new materials such as aluminum-based silicon

carbide support plate and three-point flexible support of primary mirror have successfully passed the appraisal-level vibration rest. Focusing mechanism and calibration mechanism can withstand the appraisal level test and assessment. The optical performance did not change before and after the test.



Figure 21. Vibration test photo of VT main body, Video processing box, Electric box and TEC controller box (from left to right)

4.4 Thermal test

Thermal test in ground vacuum chamber has been conducted to verify the validity of thermal design. The test results show that the CCD temperature can be controlled to $-65^{\circ}\text{C}\pm 2^{\circ}\text{C}$ with Thermo-electric coolers (TECs) and radiator. In the bake-out mode, the temperature of CCD can be controlled in $19^{\circ}\text{C}\sim 21^{\circ}\text{C}$.

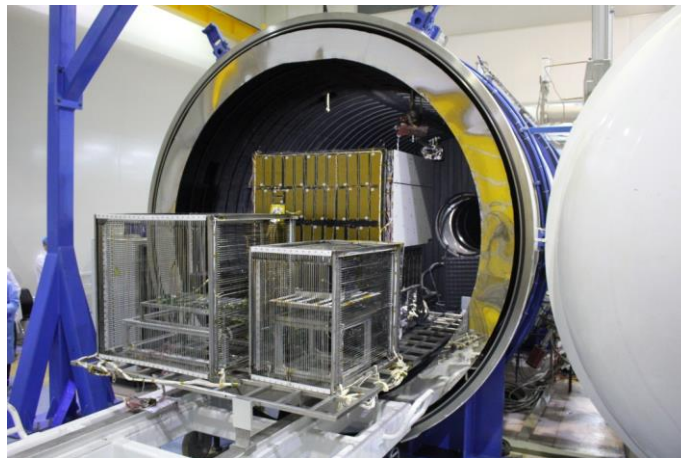


Figure 22. VT under thermal test in the vacuum chamber

5. OUTSIDE OBSERVING TEST

In order to test whether VT can achieve the scientific objectives, an outfield observation experiment was carried out at Xinglong Station, Chinese Academy of Sciences (Figure 23).

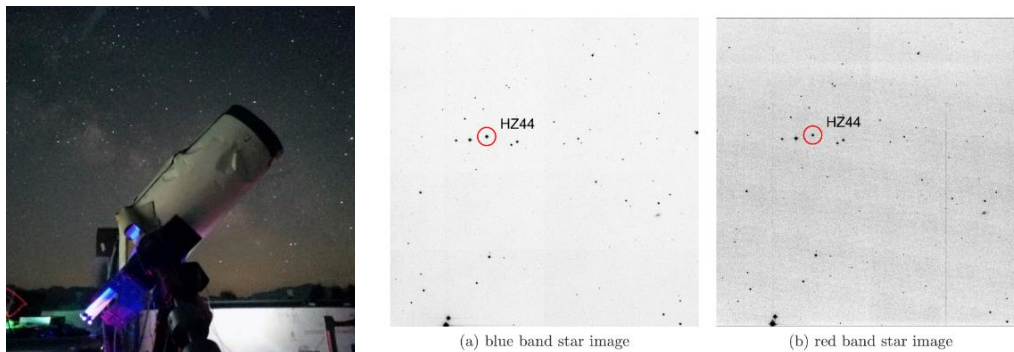


Figure 23. Left: The outfield observation experiment of VT. Right: The star Image taken by VT

The outfield observation experiment faces the problems of CCD refrigeration and atmospheric disturbance. Therefore, brighter standard stars (11-15 magnitude) were selected as Observation targets instead of 22.5 magnitude, and the on-orbit detection limit was calculated based on the observation results. At the same time of VT observation, an auxiliary telescope is used to measure the atmospheric extinction, and finally the radiation calibration and aperture photometry are performed on the VT observation results to calculate and verify the optical system efficiency and detector quantum efficiency measured in the laboratory. After determining the total efficiency of the system, the signal-to-noise ratio of each magnitude on orbit can be calculated based on the size of the spot diagrams measured in the laboratory, the predicted noise of the detector on orbit, and the value of the sky light background on orbit, and then the on-orbit detection limiting Magnitude can be finally calculated.

The results show that the average deviation between the measured value and the predicted value is about 4% in the blue band and about 5% in the red band. The outdoor observation and the on-orbit Signal-to-Noise Ratio Analysis prove that VT satisfies the scientific requirement of detecting +22.5Mv targets.

6. CONCLUSIONS

With a launch in 2021, SVOM will most probably be the main provider of accurate GRB positions in the first years of operation. In the time frame, it is envisioned that the interest in GRBs will remain high, with many important questions actively studied like: the physical mechanisms that launch the relativistic jet, the radiation processes responsible for the prompt emission, the elucidation of the connection between long GRBs and supernovae, the origin of the short/hard GRBs and of other sub-classes of GRBs like sub-energetic events and X-ray flashes. Furthermore, the quest for high redshift GRBs will continue since these events constitute valuable tools for cosmology.

VT is an important payload for the SVOM mission. The engineer model of VT has been built and tested. The EE test and PST test has shown that the telescope is able to reach the required optical performance. Low noises test shows that the electrical part can work below $5e^{-}$. VT has also passed the mechanical test and thermal test successfully. Outdoor observing experiment has proven VT can reach the limiting Magnitude +22.5Mv with the equivalent exposure time of 300s. Now the flight model of VT is under construction systematically.

REFERENCES

- [1] François Gonzalez, Shunjing Yu, "SVOM: a French/Chinese cooperation for a GRB mission," Proc. SPIE 10699, 1069920(2018).
- [2] O.Godet, J. Paul, J. Y. Wei, S.-N. Zhang, J.-L. Atteia, S. Basa, D. Barret, A.Claret, B. Cordier, J.-G. Cuby, Z. Dai, F. Daigne, J. Deng, Y. Dong, D. Götz, J.Hu, P. Mandrou, J. P. Osborne, Y. Qiu, J. Wang, B. Wu, C. Wu, W. Yuan, "The Chinese-French SVOM Mission: studying the brightest astronomical explosions," Proc. SPIE 8443, 844310(2012).
- [3] Henri Triou, Bertrand Cordier, Diego Gotz, Stéphane Schanne, Thierry Tourrette, Pierre Mandrou, Roger Pons, Olivier Godet, Nadège Remoué, Didier Barret, Jean-Luc Atteia, Martine Jouret, "The ECLAIRs telescope onboard the SVOM mission for gamma-ray burst studies," Proc. SPIE 7449, 74490X(2009).
- [4] C. Amoros, B. Houret, K. Lacombe, V. Waegebaert, J.-L. Atteia, A. Bajat, L.Bautista, I. Belkacem, S. Bordon, B. Cordier, M. Galliano, O. Godet, F.Gonzalez, Ph. Guillemot, S. Maestre, P. Mandrou, W. Marty, R. Pons, D. Rambaud, P. Ramon, "Status of technological development on ECLAIRs camera onboard the SVOM space mission," Proc. SPIE 10699, 106995K (2018).
- [5] Karine Mercier, François Gonzalez, Diego Götz, Martin Boutelier, Narjiss Boufracha, Vadim Burwitz, Marie Claire Charneau, Paul Drumm, Charlotte Feldman, Albert Gomes, Jean Michel Le Duigou, Norbert Meidinger, Aline Meuris, Paul O'Brien, Julian Osborne, Pierre Pasquier, Laurent Perraud, James F. Pearson, Frédéric Pinsard, Estelle Raynal, Richard Willingale, "MXT instrument on-board the French-Chinese SVOM mission," Proc. SPIE 10699, 1069921(2018).
- [6] Yuchen She, Shuang Li. "Optimal slew path planning for the Sino-French Space-based multiband astronomical Variable Objects Monitor mission". J. Astron. Telesc. Instrum. Syst. 4, 017001 (2018).
- [7] Peter W. A. Roming, Sally D. Hunsberger, Keith O. Mason, John A. Nousek, Patrick S. Broos, Mary J. Carter, Barry K. Hancock, Howard E. Huckle, Tom E. Kennedy, Ronnie Killough, T. Scott Koch, Michael K. McLelland, Michael S. Pryzby, Phil J. Smith, Juan Carlos Soto, Joseph Stock, Patricia T. Boyd, Martin D. Still,

- "The Swift Ultra-Violet/Optical Telescope," Proc. SPIE 5165, X-Ray and Gamma-Ray Instrumentation for Astronomy XIII, (2004).
- [8] Lee Feinberg, Lester Cohen, Bruce Dean, Willian Hayden, Joseph Howard, Ritva Keski-Kuha, "Space telescope design considerations," Opt. Eng. 51, 011006 (2012).
- [9] V. YU. TEREbizh, "OPTIMAL BAFFLE DESIGN IN A CASSEGRAIN TELESCOPE," Experimental Astronomy 11, 171-191 (2001).
- [10] M. Senthil Kumar, C. S. Narayanamurthy, A. S. Kiran Kumar, "Iterative method of baffle design for modified Ritchey-Chretien telescope", Appl. Opt. 52, 1240-1247 (2013).
- [11] Xuewu Fan, Gangyi Zou, Yulei Qiu, Zhihai Pang, Hui Zhao, Qingfang Chen, Yue Pan, Hao Yuan, "Optical design of the visible telescope for the SVOM Mission," Appl. Opt. 59, 3049-3057(2020).
- [12] John Fleming, Frank Grochocki, Tim Finch, Stew Willis, Paul Kaptchen, "New stray light test facility and initial results," Proc. SPIE 7069, 70690O (2008).
- [13] Frank Grochocki, John Fleming, "Stray light testing of the OLI Telescope," Proc. SPIE 7794, 77940W (2010).